[CANCER RESEARCH 61, 1392–1397, February 15, 2001]

Involvement of Mammalian MLH1 in the Apoptotic Response to Peroxide-induced Oxidative Stress

Rebecca A. Hardman, Cynthia A. Afshari, and J. Carl Barrett[1]

Curriculum in Toxicology, University of North Carolina, Chapel Hill, North Carolina 27514 [R. A. H., J. C. B.], and Laboratory of Molecular Carcinogenesis, National Institute of Environmental Health Sciences, Research Triangle Park, North Carolina 27709 [R. A. H., C. A. A., J. C. B.]

ABSTRACT

MLH1 is an integral part of the mismatch repair complex, and the loss of this protein is associated with the acquisition of a mutator phenotype, microsatellite instability, and a predisposition to cancer. Deficiencies in the mismatch repair complex, including the loss of MLH1, result in elevated resistance to specific inducers of DNA damage, yet the mechanisms involved in this DNA-damage resistance are largely unknown. Abnormal cellular responses to DNA damage can lead to the selection of cells with a greater propensity for neoplastic transformation and might also reduce the effectiveness of certain chemotherapeutic drugs. It is therefore important to identify agents that provide selective pressure for growth of MLH1-deficient cells and to characterize further the pathways involved. In this study, we show that both human epithelial and mouse embryo fibroblast cell lines lacking the MLH1 protein are more resistant to two inducers of oxidative stress, hydrogen peroxide and tert-butyl hydroperoxide. Our analyses suggest that the observed differences in cellular viability are mediated primarily through apoptotic pathways and not through deficiencies in cell cycle checkpoint controls. Additional characterization of the signaling pathways for hydrogen peroxide-induced apoptosis in MLH1-proficient cells demonstrates the involvement of increased mitochondrial permeability, the release of cytochrome *c*, and caspase 3 activation. Together, our data indicate that cells lacking MLH1 may possess a selective growth advantage under oxidatively stressed conditions via the disregulation of apoptosis, possibly involving the mitochondria.

INTRODUCTION

In both prokaryotic and eukaryotic cells, a highly conserved set of DNA MMR[2] enzymes is primarily responsible for the postreplicational correction of nucleotide mispairs and extra-helical loops (1). The loss of MMR genes in humans is implicated in the etiology of hereditary nonpolyposis colorectal cancer syndrome and a wide variety of sporadic tumors (2, 3). The MMR system is also involved in the cellular response to several different types of DNA damage. Human tumor cell lines deficient in MMR activity are highly resistant to the normally cytotoxic effects of MNNG, 6-TG, temozolamide, and methylnitrosourea (4–7). A more moderate-level resistance of cultured cells to chemotherapeutic agents such as cisplatin, methyl methanesulfonate, and doxorubicin is correlated with deficiencies in one or more MMR proteins, including MLH1 (8–10). The mechanisms involved in mediating the differences in cytotoxicity to these various agents are not clearly understood, but in some cases involve inadequate activation of G_2 checkpoint or apoptosis.

Recent studies in *Saccharomyces cerevisiae* have shown the involvement of MSH2/MSH6-dependent MMR in the repair of adenines misincorporated opposite the oxidatively damaged base 8-oxoguanine (11). Experiments with *mutS*-deficient *Escherichia coli* strains demonstrated the ability of the MMR system to recognize and repair exocylic DNA adducts such as those formed during endogenous lipid oxidation (12). Furthermore, mouse embryonic stem cells with defective *Msh2* alleles are more resistant to oxidative damage generated by low-level radiation (13). On the basis of this evidence, it is possible that at least a portion of the differential cytotoxicity induced by certain DNA-damaging agents is a result of variations in oxidative stress responses between MMR+ and MMR− cells. This becomes especially important considering that endogenous generation of oxidatively damaged bases is a continuous occurrence in the DNA of normal, healthy individuals (14) and also can be influenced by numerous environmental factors (15).

We designed the experiments described in this report to test the hypothesis that absence of MLH1 may provide cells with a selective growth advantage when exposed to specific forms of oxidative stress. We used both human and murine cell line pairs as model systems to study the effects of MLH1 in our experiments. The human HCT116 colon carcinoma cells have a mutant *hMLH1* gene, whereas the HCT116+3 cells contain a wild-type *hMLH1* gene introduced by the transfer of a normal human chromosome 3. The mouse MC2 embryonic fibroblasts were derived from *Mlh1*−/− knockout mice, whereas the MC5 fibroblasts have wild-type *Mlh1*. HCT 116 and MC2 cells both are deficient in MMR activity, resistant to treatment with 6-TG and MNNG and demonstrate increased microsatellite instability (5, 16, 17). The HCT 116+3 cells and the MC5 cells both have proficient MMR activity and significantly reduced microsatellite instability and also exhibit greatly increased sensitivity to both MNNG and 6-TG (17, 18).

To assess the role of MLH1 in mediating the effects of oxidative stress on cultured cells, we chose to use two well-characterized mediators of oxidative stress, H_2O_2 and TBH. H_2O_2 and TBH are known to generate a variety of different types of oxidative DNA lesions, including base modifications, frameshift mutations, and DNA strand breaks (19–21). Recent studies in *Escherichia coli* have demonstrated the ability of H_2O_2 to induce frameshift mutations preferentially in microsatellite sequences, and further show that this damage is enhanced in cells lacking MMR activity (22). Here we demonstrate that MLH1− and Mlh1− cell lines exhibit increased resistance to the cytotoxic effects of H_2O_2 and TBH compared with the MLH1+ and Mlh1+ cell lines, suggesting the involvement of MLH1 in the cellular survival response to oxidative stress. Moreover, our experiments also suggest that this resistance is the result of a requirement for MLH1 in the transduction of a mitochondrial-mediated apoptotic signal in cells exposed to peroxides.

MATERIALS AND METHODS

Cell Lines. HCT 116, a human colorectal adenocarcinoma cell line, and HCT116+3 were kindly provided by Dr. Minoru Koi (Laboratory of Molecular Carcinogenesis, National Institute of Environmental Health Sciences, Re-

Received 10/5/00; accepted 12/13/00.

The costs of publication of this article were defrayed in part by the payment of page charges. This article must therefore be hereby marked *advertisement* in accordance with 18 U.S.C. Section 1734 solely to indicate this fact.

[1] To whom requests for reprints should be addressed, at Laboratory of Molecular Carcinogenesis, National Institute of Environmental Health Sciences, Research Triangle Park, NC 27709. E-mail: barrett@mail.nih.gov.

[2] Abbreviations: MMR, mismatch repair; 6-TG, 6-thioguanine; H_2O_2, hydrogen peroxide; TBH, tert-butyl hydroperoxide; HCT116+3, HCT 116 + chromosome 3; BrdUrd, 5-bromo-2′-deoxyuridine; IR, ionizing radiation; JC-1, 5,5′,6,6′-tetrachloro-1,1′3,3′-tetraethylbenzimidazilylcarbocyanine iodide; MNNG, *N*-methyl-*N*′-nitro-*N*-nitrosoguanidine; PI, propidium iodide; PE, phycoerythrin; JNK/SAPK, c-Jun *N*-terminal kinase/stress-activated protein kinase. MTS, [3-(4,5-dimethylthiazol-2-yl)-5-(3-carboxymethoxyphenyl)-2-(4-sulfophenyl)-2*H*-tetrazolium, inner salt].

Downloaded from http://aacrjournals.org/cancerres/article-pdf/61/4/1392/3252274/ch0401013 92p.pdf by guest on 07 September 2024

search Triangle Park, NC; Ref. 5). MC2 (*Mlh1*−/−) and MC5 (*Mlh1*+/+) mouse embryo fibroblasts were kindly provided by Dr. R. M. Liskay (Oregon Health Sciences University, Portland, OR; Ref. 18). Cells were maintained in 5% CO_2 in M5 medium [DMEM/Ham's F-12 (1:1)] with 10% fetal bovine serum (Summit Biotechnologies, Ft. Collins, CO). Medium for HCT116+3 cells also included 400 μg/ml G418 (Life Technologies, Inc., Gaithersburg, MD). Unless otherwise noted, cells were plated 24 h before each treatment at a density of 400,000 cells/100 mm dish. All treatments were done in M5 medium with 10% serum.

Cytotoxicity Assessment. Cells were seeded at 4000 cells/well into 96-well plates 24 h before treatment. H_2O_2 and TBH treatments were for 1 h, and IR treatments were for <10 min to achieve 2-, 4-, 8-, 16-, and 32-Gy doses using a Cs^{137} source irradiator (J. L. Sheppard Associates). Viability was assessed 72 h after treatment using the MTS-based CellTiter96 AQ_{ueous} Non-Radioactive Cell Proliferation Assay (Promega, Madison WI) according to the manufacturer's instructions.

Cell Cycle Analysis (Dual-parameter Flow Cytometry). Cells were pulse-labeled with 10 μM BrdUrd for 20 min, harvested and processed with FITC-conjugated Anti-BrdUrd (250 ng; Becton Dickinson, San Jose, CA) according to the manufacturer's instructions, then stained with PI (final concentration 5 μg/ml) and analyzed using a FACScan flow cytometer (Becton Dickinson). Quantitative analyses and cell cycle histograms were generated using the CellQuest 3.1 software program (Becton Dickinson).

DNA Fragmentation Analysis. The floating cell population from each sample was collected at 24 h after treatment. Genomic DNA was prepared and the entire sample analyzed for laddering on a 0.8% agarose gel as described previously (23).

Microscopic Analysis of Nuclear Morphology. Cells were plated at equal densities on glass slide chambers. At 24 h after H_2O_2 treatment, the cells were fixed in methanol:acetic acid (3:1) and then stained with 20 μg/ml PI for 15 min before being analyzed using a Zeiss Axiophot fluorescent microscope coupled with a Spot CCD camera system (Olympus).

Active Caspase 3 Measurement. The entire cell population from each sample was gently harvested at 24 h after treatment, fixed, and incubated with 20 μl of PE-conjugated primary antibody to active caspase 3 (PharMingen) according to the manufacturer's instructions. The cells were rinsed in PBS and immediately analyzed on a FACSort flow cytometer using the FL1 detector with standard PE settings.

Measurement of DNA Lesion Frequency. Damage induced in nuclear DNA following a 1-h exposure to H_2O_2 and TBH was evaluated using a quantitative long PCR assay as described by Van Houten *et al.* (24), with minor modifications. Briefly, 30 ng of DNA were amplified using primers for a 13.5-kb *human β-globin* gene fragment (sense, 5′-CGAGTAAGAGACCATTGTGGCAG-3′; antisense, 5′-GCACTGGCTTAGGAGTTGGACT-3′). The single-band end products of each PCR reaction were measured using PicoGreen dsDNA quantitation reagent (Molecular Probes, Eugene, OR). The results of treated sample amplifications are presented as relative to the untreated control amplifications.

Cytochrome C Release Analysis. Cells were treated with H_2O_2 for 1 h. At 24 h after treatment, cells were gently resuspended in cytoplasmic extract buffer [1 mM EDTA, 60 mM KCl, 10 mM HEPES (pH 7.5), 0.5% NP40, 1 mM phenylmethylsulfonyl fluoride, 1 mM DTT, and 1 × pepstatin/leupeptin], iced for 30 min, and homogenized by pulling 10 times through a 25-gauge needle. Nuclei and cell debris were pelleted by centrifugation at 14,000 × *g*, and 25 μg of each extract was separated on a 15% SDS-PAGE gel for Western analysis using anti-cytochrome *c* antibody (PharMingen) at a 1:200 dilution with enhanced chemiluminescence (Amersham) detection.

Assessment of Mitochondrial Permeability. At 24 h after 1-h treatment with H_2O_2, each sample was resuspended in 5 ml of prewarmed (37°C) medium. A 1-ml aliquot was incubated with 1 μg/ml of the cationic dye JC-1 (Molecular Probes, Eugene, OR) for 30 min at 37°C and then analyzed using a conventional flow cytometer with simultaneous FL1 (green/525 nm) and FL2 (red/590 nm) fluorescence detection. Both parameters are represented on a density contour plot of each sample population. Quantitative estimations of JC-1 monomer formation based on gating of the population gaining FL1 fluorescence in three separate experiments are given in the *lower right corner* of each frame in Fig. 7.

RESULTS

MLH1-deficient Cells Have Increased Resistance to Cytotoxic Effects of Peroxides. To determine whether or not MLH1 could be a factor in oxidative stress-mediated cytotoxicity, we compared the relative sensitivities of MLH1-proficient and MLH1-deficient cell lines to both H_2O_2 and TBH. Using a standard MTS-based cellular viability assay, all cell lines demonstrated a dose-dependent sensitivity to H_2O_2 exposure at 72 h after treatment (Fig. 1*A*). However, the level of sensitivity was significantly greater in the HCT116+3 (MLH1+) and MC5 (Mlh1+) cell lines when compared with that of their repair-deficient counterparts. At a dose of 400 μM H_2O_2, the mean viability of the HCT116+3 cell line was 51%, whereas the mean viability of the HCT116 cell line was 78%. Confirmation of these results was obtained using a colony-forming assay in which the HCT116+3 cells had ~10% and HCT116 cells had 60% colony forming at the 400 μM dose (data not shown).

Because H_2O_2 is unstable, we also used TBH to generate reactive oxygen species and evaluated its cytotoxic effects in our model systems. TBH induced greater cytotoxicity than H_2O_2, probably because of the fact that it is not as efficiently metabolized. Similar to the results seen with H_2O_2, the repair-deficient HCT116 (MLH1−) and MC2 (Mlh1−) cells were more resistant to the cytotoxic effects of TBH (Fig. 1*B*). Because current reports of MMR involvement in the repair of IR-induced lesions are contradictory, we also evaluated the responses in our model system to IR, a commonly used model for the induction of oxidative stress. All four cell lines exhibited a similar response to IR, regardless of MMR status. This is perhaps because IR induces a much higher level of double-strand breaks and comparatively less base damage than do either of the peroxides. From these results, we conclude that the presence of MLH1 or Mlh1 increases

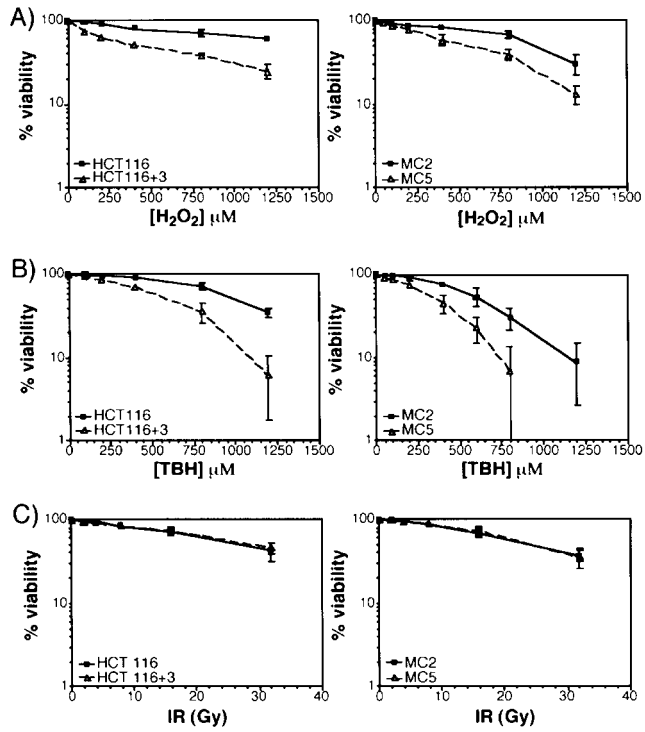

Fig. 1. Cell viability in MLH1+ and MLH1− cell lines after treatment with oxidative stressors. Human HCT116 (MLH1−) and HCT116+3 (MLH1+) cells and mouse MC2 (Mlh1−/−) and MC5 (Mlh1+/+) cells treated for 1 h with H_2O_2 (*A*), TBH (*B*), and IR (*C*). Treatments were followed by a 72-h incubation in normal growth medium, at which time cellular viability was determined using the MTS assay. Results are shown as the percentage of mock-treated control and represent the mean ± SD of three separate experiments.

Downloaded from http://aacrjournals.org/cancerres/article-pdf/61/4/1392/3252274/ch0401013392p.pdf by guest on 07 September 2024

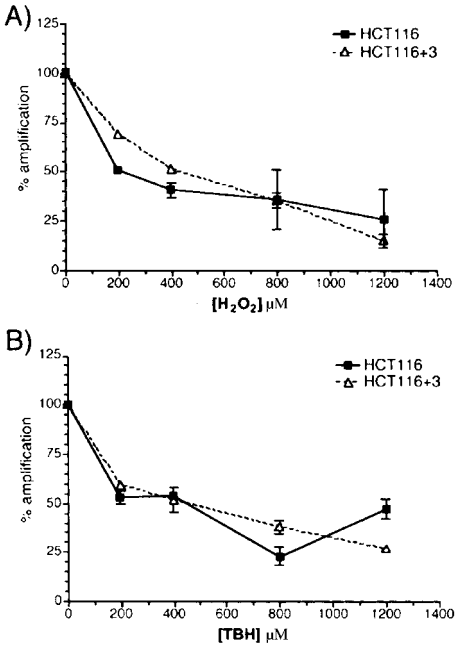

Fig. 2. Analysis of DNA lesion frequencies in nuclear DNA after treatment with H_2O_2 and TBH. Total genomic DNA was isolated from HCT116 and HCT16+3 cells immediately after a 1-h treatment with H_2O_2 (*A*) and TBH (*B*). Using a quantitative PCR technique described by Van Houten *et al.* (24), a 13.5-kb β-globin fragment was amplified from each sample. The ability of the nuclear β-globin fragment to amplify in treated *versus* control samples (percentage amplification) is directly proportional to the amount of polymerase-blocking DNA damage present (lesion frequency).

sensitivity to peroxide-induced oxidative stress, but has a negligible effect on survival after high-dose IR.

We next wanted to eliminate the possibility that differences in DNA damage dosing were mediating the observed cytotoxicity differences. To determine the relative amounts of DNA damage delivered to each cell line during treatment with peroxides, we used a quantitative long PCR assay designed to measure induced levels of polymerase-blocking DNA damage (24). As shown in Fig. 2, there were no significant differences observed between the HCT116 and HCT116+3 cell lines in the initial amounts of DNA damage generated during a 1-h exposure to increasing doses of either H_2O_2 or TBH. Furthermore, analysis of damage levels at several time points after treatment showed no significant differences, suggesting that the repair of polymerase-blocking DNA damage between the two cell lines is similar (data not shown). This suggests that the greater sensitivity of the HCT116+3 cell line to peroxides is not attributable to an increased initial DNA damage load placed on the cell.

Cell Cycle Checkpoint Function after Peroxide Treatment Is Independent of MMR Status. The MLH1 protein is involved in the G_2-M cell cycle checkpoint after exposure to 6-TG, MNNG, and IR, although the mechanisms and extent of MLH1 involvement are unknown (6, 18, 25, 26). To determine whether MLH1 affects the integrity of cell cycle checkpoints after peroxide treatment, we performed cell cycle profile analyses. As seen in Fig. 3*A* and *B*, the results indicated that, regardless of MLH1 status, a significant portion of the treated cells exhibited reduced DNA synthesis and accumulated in the late S and G_2-M compartments of the cell cycle in a dose-dependent manner. For example, gating of cells on BrdUrd/PI dot plots of the 200 μM H_2O_2 samples showed that HCT116 contained an average of 54% of cells in G_2-M and HCT116+3 contained an average of 48% of cells in G_2-M. The reduction of G_2-M content in the HCT116+3 cells at higher doses of each peroxide correlated with cell death, as evidenced by the increased sub-2N DNA content.

As seen in Fig. 3*C*, the HCT116+3 cells exhibited a significant dose-dependent increase at 24 h in the percentage of sub-2N DNA content after a 1-h exposure to either peroxide. The HCT116 cells only show elevated sub-2N DNA content after high doses of TBH, but still significantly less than that seen in the HCT116+3 cells. This is in agreement with the cytotoxicity of TBH seen at these doses (Fig. 1*B*). Overall, the analysis of cell cycle profiles provided little proof of variations in the integrity of cell cycle checkpoints after peroxide exposure. The quantitative analysis of cellular degradation, coupled with simple visual observation of treated cell cultures, suggested instead that levels of cell death were the most likely factor contributing to the observed differences in cytotoxicity.

Sensitivity to Peroxides in MLH1-proficient Cells Is Attributable to Induction of an Apoptotic Pathway. In an effort to understand better the basis for the differential cytotoxicity, we set out to determine the mode of cell death incurred after peroxide exposure in both the MLH1+ and MLH1− cell lines. DNA was isolated from floating HCT116 and HCT116+3 cells grown in 100 mM dishes after exposure to H_2O_2 and TBH and analyzed for the presence of ladder-like 180-bp DNA fragmentation characteristic of cells undergoing apoptosis. DNA ladders and floating cell populations were observed in the HCT116+3 cells, both increasing in a dose-dependent manner with each peroxide (Fig. 4*A*). No evidence of ladders was seen in the HCT116 cells after H_2O_2 or TBH treatment, and only the highest doses of TBH initiated significant levels of floating cells. As shown in Fig. 4*B*, additional data supporting the presence of apoptotic cells in the HCT116+3 cell line was obtained through observation of nuclear morphology in each cell line after exposure to H_2O_2. By staining the cells with PI, we observed condensed and fragmented nuclei indicative of apoptotic cellular events in the HCT116+3 cells, whereas the

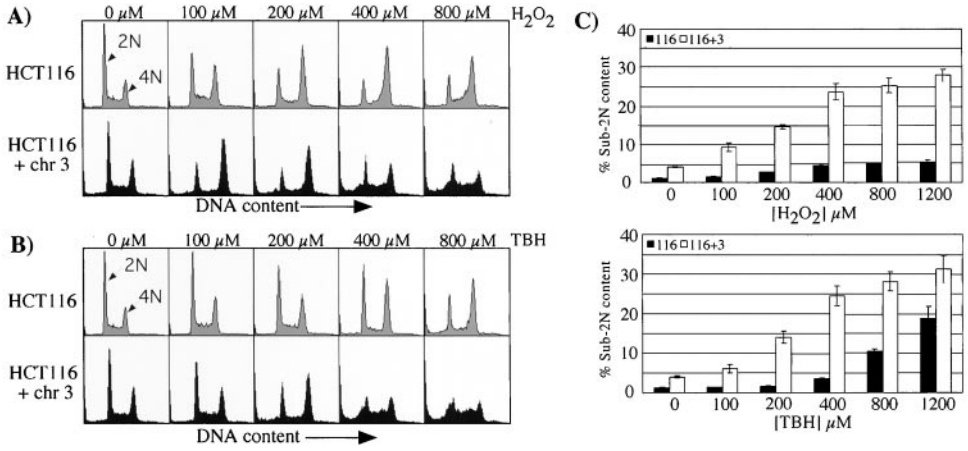

Fig. 3. Cell cycle analysis after treatment with H_2O_2 and TBH. DNA content histograms of human colon carcinoma HCT116 and HCT116+3 cells 24 h after a 1-h treatment with either H_2O_2 (*A*) or TBH (*B*). Percentage of sub-2N population (*C*) after treatment was determined using CellQuest analysis software (Becton Dickinson) and represents the mean ± SD of three separate experiments.

Downloaded from http://aacrjournals.org/cancerres/article-pdf/61/4/1392/3252274/ch0401013 92p.pdf by guest on 07 September 2024

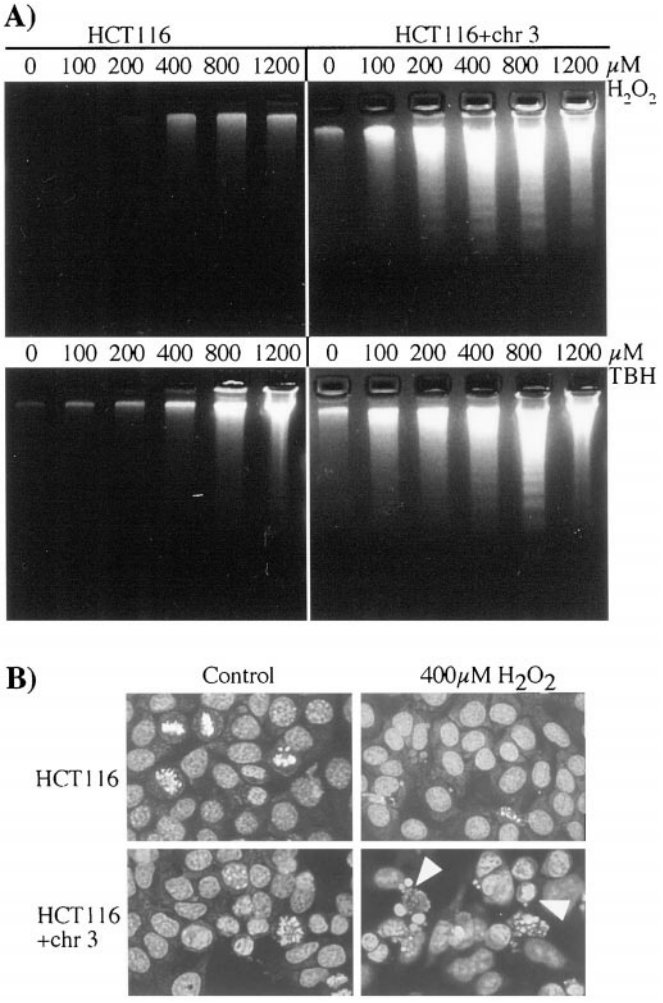

Fig. 4. Analysis of DNA fragmentation and nuclear morphology after treatment with peroxides. *A*, HCT116 and HCT116+3 cells were treated with 0–1200 μM H_2O_2 or TBH for 1 h, given fresh media, and the floating cell population was harvested and pelleted 24 h after treatment. Genomic DNA isolated from the entire sample was analyzed on a 2% agarose gel. *B*, HCT116 and HCT116+3 cells plated at equal densities on glass culture slides were treated with 400 μM H_2O_2 for 1 h. Slides were fixed 24 h after treatment and stained with PI to allow visualization of nuclei at ×1000.

HCT116 cells displayed little if any evidence of morphology characteristic of apoptotic cell death.

Characterization of MLH1-associated Apoptosis after Peroxide Exposure. In the apoptotic cascade of events, the upstream mediators of both nuclear condensation and DNA fragmentation are triggered by the presence of active caspase 3 (27). After peroxide treatment, we measured levels of active caspase 3 using a PE-conjugated antibody that selectively recognizes only the active form of this caspase. In agreement with the increases in cell death and DNA laddering observed in the HCT116+3 cell line after exposure to H_2O_2 and TBH, we saw an induction of active caspase 3 in this cell line (Fig. 5). Likewise, the resistant HCT116 cells demonstrated little activation of caspase 3, only being induced at the highest doses of TBH. This data suggests a role for MLH1 in triggering apoptosis that includes, but also is upstream of, caspase 3 signaling.

One of the primary pathways through which activation of caspase 3 is known to occur involves the release of cytochrome *c* from the mitochondria (28). Cytosolic cytochrome *c* binds to Apaf-1, resulting in the activation of caspase 9 and triggering a cascade of proteolytic events, including activation of caspase 3, leading to apoptosis (29). To determine whether cytochrome *c* release might be occurring after peroxide treatment, we analyzed cytoplasmic extracts from H_2O_2-treated HCT116 and HCT116+3 by Western blotting. Fig. 6 shows the detection of increased cytochrome *c* in the HCT116+3 extracts at both the 400- and 800-μM H_2O_2 doses at 24 h post-treatment. Similar results exhibiting weaker bands were also observed at 6 h after treatment with the same doses (data not shown). No significant increases in cytochrome *c* were detected in cytoplasmic extracts from identically treated HCT116 cells at either time point. These results suggest that cytochrome *c* release may be an important part of the peroxide-induced apoptotic pathway in MLH1+ cells.

Cytochrome *c* release from the mitochondria can be triggered with or without loss of mitochondrial inner transmembrane potential ($\Delta\Psi$m) through the formation of pores transversing both the inner and outer mitochondrial membranes (30, 31). To determine the role of mitochondrial permeability in the release of cytochrome *c* in HCT116+3 cells, we incubated live cells with the cationic dye JC-1 and observed the resulting fluorescence using dual-parameter flow cytometry. JC-1 selectively accumulates in mitochondria in a $\Delta\Psi$m dependent manner where it forms red fluorescing J-aggregates. In untreated cells from both cell lines, the majority of JC-1 appears in its red (~590 nm) fluorescing dimer form after being taken up by the mitochondria (Fig. 7). A significant dose-dependent appearance of green (~525 nm) fluorescing (nondimerized) cytoplasmic JC-1 molecules was observed in the HCT116+3 cells after H_2O_2 exposure, indicating an increase in the permeability of the mitochondria. Across each of the doses tested, the cytoplasmic JC-1 fluorescence in

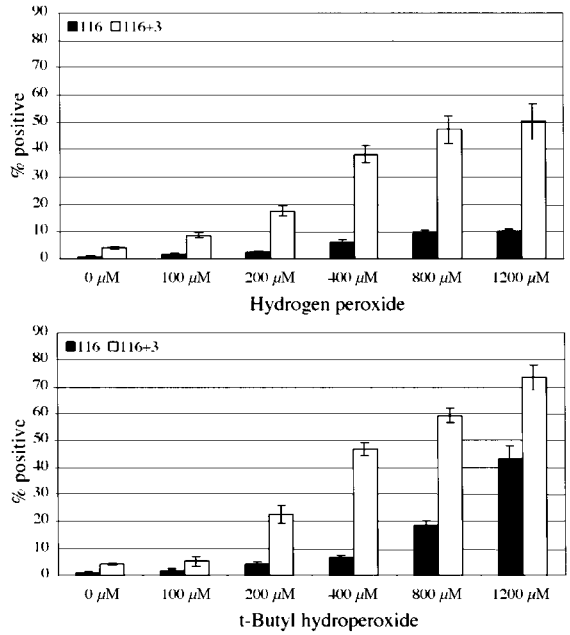

Fig. 5. Measurement of active caspase 3 levels. HCT116 and HCT116+3 cells were treated with 0–1200 μM H_2O_2 or TBH for 1 h. All cells from each dish were collected and fixed 24 h after treatment, and active caspase 3 was detected using a PE-conjugated antibody. Quantitative determination of the population positive for active caspase 3 was done by flow cytometric analysis and represents the mean ± SD for three separate experiments.

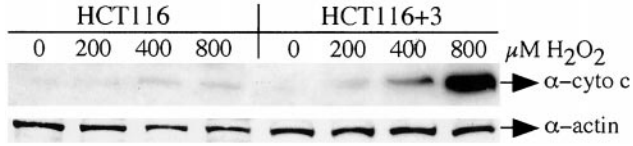

Fig. 6. Cytochrome *c* release. Cytoplasmic protein extract was collected from HCT116 and HCT116+3 cells 24 h after a 1-h treatment with H_2O_2 and analyzed for cytochrome *c* content by Western blotting. β-actin antibody reactivity is shown as a loading control.

Downloaded from http://aacrjournals.org/cancerres/article-pdf/61/4/1392/3252274/ch0401013392p.pdf by guest on 07 September 2024

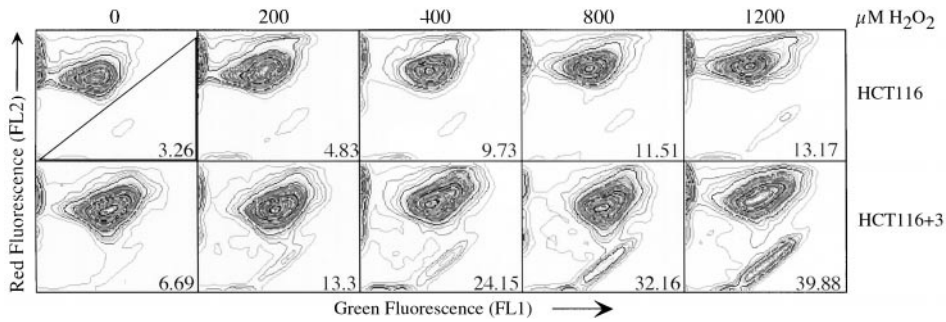

Fig. 7. Induction of mitochondrial permeability. Fluorescence of JC-1 was determined in live cells 24 h after a 1-h treatment with H_2O_2. Cells were incubated with JC-1 before analysis on a fluorescence-activated cell sorting flow cytometer using both the FL1 (*green*, 525 nm) and FL2 (*red*, 590 nm) detectors simultaneously. Dose-dependent loss of JC-1 from the mitochondria is reflected by the loss of FL2-detected events in conjunction with an increase in FL1detected events. Numbers in the *bottom right corner* of each frame represent the mean percentage of FL1 events in each population from three separate experiments.

HCT116+3 cells was significantly higher than in the HCT116 cells. This indicates that loss of $\Delta\Psi$m in MLH1+ cell lines may be an important factor in the initiation or execution of peroxide-induced apoptosis.

DISCUSSION

Our results using both human and murine cell pairs as a model system clearly demonstrate a role for MLH1/Mlh1 in mediating cellular sensitivity to the peroxides H_2O_2 and TBH. Reports by Hawn *et al.* and others (6, 17, 18) demonstrated deficiencies in cell cycle checkpoint capabilities (specifically the G_2-M checkpoint) in MLH1− cell lines after DNA damage induced by agents such as MNNG and 6-TG or by various chemotherapeutics. Unlike these studies, we see similar induction of a late S and G_2-M cell cycle delay after peroxide exposure, regardless of MLH1 status. Our experiments suggest that the sensitivity to peroxides in the MLH1+ and Mlh1+/+ cells is attributable instead to elevated levels of cell death.

Previous studies have indicated a role for *Msh2* in the apoptotic response to protracted low-level radiation-induced oxidative stress in murine embryonic fibroblasts (13). Mice with homozygous deletions of *Msh2* were used to demonstrate a role *in vivo* for Msh2 in the regulation of apoptosis in the small intestine (32). Also, microinjection of plasmids containing *hMLH1* or *hMSH2*, but not *hPMS2*, *hMSH3*, and *hMSH6*, induces apoptosis in both repair-proficient and -deficient cell lines (11). Our results support and extend the previous findings by demonstrating the involvement of the MLH1 protein in mediating cellular sensitivity to peroxide-induced oxidative stress via regulation of apoptosis. An important observation supported throughout our work is that with normal background damage levels, the MLH1+ cells exhibit higher levels of apoptosis when compared with MLH1− cells. Therefore, altered regulation of MLH1 expression could be a factor in triggering cell death even under steady-state levels of DNA damage.

A growing body of evidence links the MMR proteins MLH1 and MSH2 to the apoptotic process, yet little is known about the mechanisms through which this might occur. Recent data suggests that MMR competency is required for initiation of an apoptotic response to methylating agents through a pathway thought to involve the p53 tumor suppressor protein (6, 32–34). Much less is known about the pathways involved in the lower-level resistance to such agents as cisplatin and oxidative stress, but they appear to differ from those of the methylators (35–37). Key initiators of the apoptotic cascade in most mammalian cell types include the loss of mitochondrial membrane integrity and the subsequent release of cytochrome *c*. Cytochrome *c* release from mitochondria after the exposure of cultured cells to such DNA-damaging agents as IR, cisplatin, and methyl methanesulfonate has been documented previously (38). In our study, we observed both increased mitochondrial permeability and cytochrome *c* release after H_2O_2 treatment preferentially in the more sensitive MLH1+ cell line. This suggests that sensitivity to peroxides may be mediated by MLH1 through an apoptotic signal transduction pathway involving the mitochondria.

JNK/SAPK signal transduction pathways are activated after exposure to oxidative stressors, including peroxides (39). Recent evidence has shown that JNK/SAPK can be activated by genotoxic stressors to translocate to the mitochondria and phosphorylate Bcl-x_L at specific Thr-Pro sites (38). Phosphorylation of Bcl-x_L is subsequently hypothesized to promote cytochrome *c* translocation and lead to the induction of apoptosis. Nehmé *et al.* (37) reported that MMR-proficient cells activate JNK more efficiently after cisplatin treatment than MMR-deficient cells, and only MMR-proficient cells are able to activate c-Abl. On the basis of these observations, it is intriguing to speculate that the difference in ability of MLH1+ and MLH1− cell lines to undergo apoptosis after exposure to peroxides might be linked to the activation of JNK/SAPK pathways, possibly through their ability to regulate Bcl-2 family members.

Collectively, our work demonstrates that MLH1− and Mlh1− cell lines exhibit increased resistance to the cytotoxic effects of H_2O_2 and TBH compared with their MLH1+ and Mlh1+ counterparts, suggesting the involvement of MLH1 in the cellular survival response to oxidative stress. Moreover, our experiments also suggest that this resistance is the result of a requirement for MLH1 in the transduction of a mitochondrial-mediated apoptotic signal in cells exposed to peroxides. Given the extensive nature of endogenously generated oxidative DNA damage (15), this work may hold important implications for understanding the evolution of both sporadic and hereditary tumors of the MMR− phenotype and might prove useful in the development of targeted chemotherapeutic strategies for patients with MMR-deficient tumors.

ACKNOWLEDGMENTS

We thank Drs. Minoru Koi and Michael Liskay for sharing their cell lines and also Yiming Chen and Dr. Bennett Van Houten for assistance with the QPCR assay. We also thank Drs. Alex Merrick and John Risinger for critical review of this manuscript.

REFERENCES

1. Kolodner, R. D., and Marsischky, G. T. Eukaryotic DNA mismatch repair. Curr. Opin. Genet. Dev., *9:* 89–96, 1999.
2. Lynch, H. T., Smyrk, T., and Lynch, J. F. Overview of natural history, pathology, molecular genetics and management of HNPCC (Lynch Syndrome). Int. J. Cancer, *69:* 38–43, 1996.
3. Fishel, R., and Kolodner, R. D. Identification of mismatch repair genes and their role in the development of cancer. Curr. Opin. Genet. Dev., *5:* 382–395, 1995.
4. Branch, P., Hampson, R., and Karran, P. DNA mismatch binding defects. Cancer Res., *55:* 2304–2309, 1995.
5. Koi, M., Umar, A., Chauhan, D. P., Cherian, S. P., Carethers, J. M., Kunkel, T. A., and Boland, C. R. Human chromosome 3 corrects mismatch repair deficiency and microsatellite instability and reduces *N*-methyl-*N*′-nitro-*N*-nitrosoguanidine tolerance in colon tumor cells with homozygous *hMLH1*. Cancer Res., *54:* 4308–4312, 1994.

Downloaded from http://aacrjournals.org/cancerres/article-pdf/61/4/1392/3252274/ch0401013392p.pdf by guest on 07 September 2024

6. D'Atri, S., Tentori, L., Lacal, P. M., Graziani, G., Pagani, E., Benincasa, E., Zambruno, G., Bonmassar, E., and Jiricny, J. Involvement of the mismatch repair system in temozolomide-induced apoptosis. Mol. Pharmacol., *54:* 334–341, 1998.
7. Humbert, O., Fiumicino, S., Aquilina, G., Branch, P., Oda, S., Zijno, A., Karran, P., and Bignami, M. Mismatch repair and differential sensitivity of mouse and human cells to methylating agents. Carcinogenesis (Lond.), *20:* 205–214, 1999.
8. Drummond, J. T., Anthoney, A., Brown, R., and Modrich, P. Cisplatin and Adriamycin resistance are associated with MutLα and mismatch repair deficiency in an ovarian tumor cell line. J. Biol. Chem., *271:* 19645–19648, 1996.
9. Glaab, W. E., Risinger, J. I., Umar, A., Barrett, J. C., Kunkel, T. A., and Tindall, K. R. Cellular resistance and hypermutability in mismatch repair-deficient human cancer cell lines following treatment with methyl methanesulfonate. Mutat. Res., *398:* 197–207, 1998.
10. Fink, D., Nebel, S., Norris, P. S., Aebi, S., Kim, H. K., Haas, M., and Howell, S. B. The effect of different chemotherapeutic agents on the enrichment of DNA mismatch repair-deficient tumor cells. Br. J. Cancer, *77:* 703–708, 1998.
11. Ni, T. T., Marsischky, G. T., and Kolodner, R. D. MSH2 and MSH6 are required for removal of adenine misincorporated opposite 8-oxo-guanine in *S. cerevisiae*. Mol. Cell, *4:* 439–444, 1999.
12. Johnson, K. A., Mierzwa, M. L., Fink, S. P., and Marnett, L. J. MutS recognition of exocyclic DNA adducts that are endogenous products of lipid oxidation. J. Biol. Chem., *274:* 27112–27118, 1999.
13. DeWeese, T. L., Shipman, J. M., Larrier, N. A., Buckley, N. M., Kidd, L. R., Groopman, J. D., Cutler, R. G., te Riele, H., and Nelson, W. G. Mouse embryonic stem cells carrying one or two defective *Msh2* alleles respond abnormally to oxidative stress inflicted by low-level radiation. Proc. Natl. Acad. Sci. USA, *95:* 11915–11920, 1998.
14. Bohr, V. A., and Anson, R. M. DNA damage, mutation, and fine structure DNA repair in aging. Mutat. Res., *338:* 25–34, 1995.
15. Ames, B. N., Gold, L. S., and Willett, W. C. The causes and prevention of cancer. Proc. Natl. Acad. Sci. USA, *92:* 5258–5265, 1995.
16. Umar, A., Boyer, J. C., Thomas, D. C., Nguyen, D. C., Risinger, J. I., Boyd, J., Ionov, Y., Perucho, M., and Kunkel, T. A. Defective mismatch repair in extracts of colorectal and endometrial cancer cell lines exhibiting microsatellite instability. J. Biol. Chem., *269:* 14367–14370, 1994.
17. Hawn, M. T., Umar, A., Carethers, J. M., Marra, G., Kunkel, T. A., Boland, C. R., and Koi, M. Evidence for a connection between the mismatch repair system and the G_2 cell cycle checkpoint. Cancer Res., *55:* 3721–3725, 1995.
18. Buermeyer, A. B., Wilson-Van Patten, C., Baker, S. M., and Liskay, R. M. The human MLH1 cDNA complements DNA mismatch repair defects in Mlh1-deficient mouse embryonic fibroblasts. Cancer Res., *59:* 538–541, 1999.
19. Altman, S. A., Zastawny, T. H., Randers, L., Lin, Z., Lumpkin, J. A., Remacle, J., Dizdaroglu, M., and Rao, G. tert.-butyl hydroperoxide-mediated, DNA base damage in cultured mammalian cells. Mutat. Res., *306:* 35–44, 1994.
20. Halliwell, B., and Aruoma, O. I. DNA damage by oxygen-derived species. FEBS Lett., *281:* 9–19, 1991.
21. Rodriguez, H., and Akman, S. A. Mapping oxidative DNA damage at nucleotide level. Free Radic. Res., *29:* 499–510, 1998.
22. Jackson, A. L., Chen, R., and Loeb, L. A. Induction of microsatellite instability by oxidative DNA damage. Proc. Natl. Acad. Sci. USA, *95:* 12468–12473, 1998.
23. Chiao, C., Carothers, A. M., Grunberger, D., Solomon, G., Preston, G. A., and Barrett, J. C. Apoptosis and altered redox state induced by caffeic acid phenethyl ester (CAPE) in transformed rat fibroblast cells. Cancer Res., *55:* 3576–3583, 1995.
24. Van Houten, B., Chen, Y., Nicklas, J. A., Rainville, I. R., and O'Neill, J. P. Development of long PCR techniques to analyze deletion mutations of the human *hprt* gene. Mutat. Res., *403:* 171–175, 1998.
25. Carethers, J. M., Hawn, M. T., Chauhan, D. P., Luce, M. C., Marra, G., Koi, M., and Boland, C. R. Competency in mismatch repair prohibits clonal expansion of cancer cells treated with *N*-methyl-*N*′-nitro-*N*-nitrosoguanidine. J. Clin. Investig., *98:* 199–206, 1996.
26. Davis, T. W., Wilson-Van Patten, C., Meyers, M., Kunugi, K. A., Cuthill, S., Reznikoff, C., Garces, C., Boland, C. R., Kinsella, T. J., Fishel, R., and Boothman, D. A. Defective expression of the DNA mismatch repair protein, MLH1, alters G_2-M cell cycle checkpoint arrest following ionizing radiation. Cancer Res., *58:* 767–778, 1998.
27. Green, D. R. Apoptotic pathways: the roads to ruin. Cell, *94:* 695–698, 1998.
28. Wolf, B. B., and Green, D. R. Suicidal tendencies: apoptotic cell death by caspase family proteinases. J. Biol. Chem., *274:* 20049–20052, 1999.
29. Cai, J., Yang, J., and Jones, D. P. Mitochondrial control of apoptosis: the role of cytochrome c. Biochim. Biophys. Acta, *1366:* 139–149, 1998.
30. Yang, J. C., and Cortopassi, G. A. Induction of the mitochondrial permeability transition causes release of the apoptogenic factor cytochrome c. Free Radic. Biol. Med., *24:* 624–631, 1998.
31. Jürgensmeier, J. M., Xie, Z., Deveraux, Q., Ellerby, L., Bredesen, D., and Reed, J. C. Bax directly induces release of cytochrome C from isolated mitochondria. Proc. Natl. Acad. Sci. USA, *95:* 4997–5002, 1998.
32. Toft, N. J., Winton, D. J., Kelly, J., Howard, L. A., Dekker, M., te Riele, H., Arends, M. J., Wyllie, A. H., Margison, G. P., and Clarke, A. R. Msh2 status modulates both apoptosis and mutation frequency in the murine small intestine. Proc. Natl. Acad. Sci. USA, *96:* 3911–3915, 1999.
33. Hickman, M. J., and Samson, L. D. Role of DNA mismatch repair and p53 in signaling induction of apoptosis by alkylating agents. Proc. Natl. Acad. Sci. USA, *96:* 10764–10769, 1999.
34. Duckett, D. R., Bronstein, S. M., Taya, Y., and Modrich, P. hMutSα- and hMutLα-dependent phosphorylation of p53 in response to DNA methylator damage. Proc. Natl. Acad. Sci. USA, *96:* 12384–12388, 1999.
35. Vikhanskaya, F., Colella, G., Valenti, M., Parodi, S., D'Incalci, M., and Broggini, M. Cooperation between p53 and hMLH1 in a human colocarcinoma cell line in response to DNA damage. Clin. Cancer Res., *5:* 937–941, 1999.
36. Gong, J. G., Costanzo, A., Yang, H. Q., Melino, G., Kaelin, W. G. J., Levrero, M., and Wang, J. Y. The tyrosine kinase c-Abl regulates p73 in apoptotic response to cisplatin-induced DNA damage. Nature (Lond.), *399:* 806–809, 1999.
37. Nehmé, A., Baskaran, R., Nebel, S., Fink, D., Howell, S. B., Wang, J. Y., and Christen, R. D. Induction of JNK and c-Abl signalling by cisplatin and oxaliplatin in mismatch repair-proficient and -deficient cells. Br. J. Cancer, *79:* 1104–1110, 1999.
38. Kharbanda, S., Pandey, P., Schofield, L., Israels, S., Roncinske, R., Yoshida, K., Bharti, A., Yuan, Z. M., Saxena, S., Weichselbaum, R., Nalin, C., and Kufe, D. Role for Bcl-xL as an inhibitor of cytosolic cytochrome C accumulation in DNA damage-induced apoptosis. Proc. Natl. Acad. Sci. USA, *94:* 6939–6942, 1997.
39. Wang, X., Martindale, J. L., Liu, Y., and Holbrook, N. J. The cellular response to oxidative stress: influences of mitogen-activated protein kinase signaling pathways on cell survival. Biochem. J., *333:* 291–300, 1998.

Downloaded from http://aacrjournals.org/cancerres/article-pdf/61/4/1392/3252274/ch0401013392p.pdf by guest on 07 September 2024